Transactions of the JWRI, **30** (2001), 167-172

WETTING AND INTERFACE INTEGRITY OF Sn-Ag-Bi SOLDER/Fe-42%Ni ALLOY SYSTEM

C-W. Hwang*, K. Suganuma*, E. Saiz**, and A. P. Tomsia**
* Institute of Scientific and Industrial Research, Osaka University, JAPAN
** Lawrence Berkeley National Laboratory, Berkeley, CA, USA

ABSTRACT

The wetting and interfacial integrity of lead-free Sn-Ag and Sn-Ag-Bi solders with 42 alloy (Fe-42wt% Ni) were investigated. A tin-iron intermetallic layer formed at the interface and, during cooling, Ni_3Sn_4 platelets precipitated in the solder. After bonding, the Sn-3Ag joints have a eutectic microstructure, with a fine network of Ag_3Sn particles surrounding large primary β-Sn grains. Bismuth addition to Sn-3Ag improved wettability, but decreased the joint strength, owing to Bi segregation to the interface.

1. INTRODUCTION

Sn-Ag alloys are expected to be one of the best candidates for lead-free solders. They have good mechanical properties, and the soldered joints have a eutectic microstructure (consisting of a network of fine Ag_3Sn particles surrounding primary β-Sn grains) that exhibits excellent structural integrity [1]. Previous research has established that the addition of Bi to the Sn-Ag alloys decreases the melting temperature and increases their tensile strength [2]. However, the bonding between Sn-Ag-Bi solders and the alloys typically used as electrode material in electronic devices (such as the 42 alloy, Fe-42wt% Ni) is not fully understood yet. The purpose of the present work is to evaluate the wetting and interface microstructure between Sn-Ag-Bi solders and the 42 alloy, focusing on the effect of bismuth addition.

2. EXPERIMENTAL PROCEDURE

Tin and Sn-3 wt% Ag-Bi solder ingots with 0, 3 and 6 wt% Bismuth (Senju Metals Co., Ltd, Japan) were used to bond 42-alloy rods (15 mm in diameter, 15 mm in height). Before bonding, the ingots were cold-rolled into 250 μm thick sheets, and the bonding faces of the rods were polished to optical flatness with 0.3 μm Al_2O_3 powders. Soldering was performed by placing solder sheets between two 42-alloy rods under 0.5 MPa uniaxial pressure and heating at temperatures between 250─300°C for 3600 seconds. To maintain uniform thickness through the solder layer, Mo wires (200 μm in diameter) were used as spacers (Figure 1). Rosin-activated flux (RA type), containing 0.029 wt% hydrochloric acid in isopropanol alcohol, was applied to prevent oxidation during soldering.

Corresponding author: K. Suganuma, Institute of Scientific and Industrial Research, Osaka University, JAPAN. Fax No: 81-6-879-8522. E-mail: suganuma@isir2.sanken.osaka-u.ac.jp

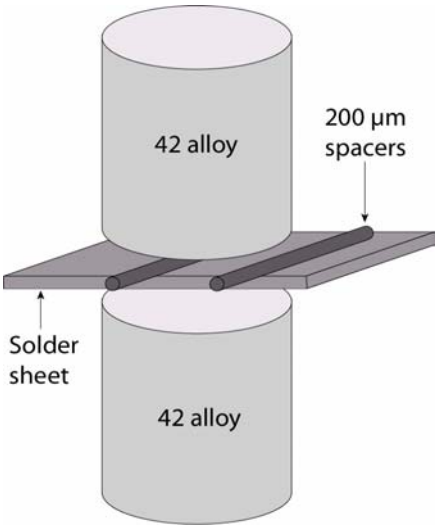

Figure 1. Joining set up

After bonding, bars (1 mm × 3 mm × 30 mm) were cut from the rods to measure the tensile strength of the bonds. The tensile tests were performed with a crosshead speed of 0.5 mm/min. Before the strength test, several bars were aged at 125ºC for times up to 500 hours to evaluate the interfacial stability. The microstructure and phase distribution in the joints were examined by optical microscopy, scanning electron microscopy (SEM), electron microprobe analysis (EPMA), energy dispersive x-ray spectroscopy (EDS) and x-ray diffraction (XRD). Table 1 shows each soldering condition and evaluation.

We studied the spreading of Sn-Ag-Bi solders on 42 alloy using a drop-transfer set-up inside a furnace heated with a W resistance in flowing Ar/H_2 (95/5 %). To facilitate the tests, we placed the solder drops on Al_2O_3 plates and heated them up to 500°C. At this temperature, the drop is shiny, suggesting that the surface oxide was effectively removed. After holding at 500ºC for 30 minutes, we cooled the furnace to 250ºC, and a polished 42 alloy plate was slowly moved towards the top of the molten drop until it just touched the liquid. The spreading of the solder on the alloy was then recorded using a high-speed camera (having the capability of 500 frames per second).

Table 1. Soldering Conditions and Evaluation

Solder	**Electrode**	**Condition**	**Evaluation**
Sn	42 alloy	Temperature: 250, 300ºC Time: 3600 sec	-Microstructure - Reaction layer
Sn-3Ag			
Sn-3Ag-(0, 3, 6) Bi	42 alloy	Temperature: 250ºC	- Wettability
	42 alloy with or without Sn plating	Temperature: 250ºC Time: 30 sec	- Microstructure - Tensile test

3. RESULTS AND DISCUSSION

3.1 Microstructure of Sn and Sn-3Ag solder/42 alloy joints

Figure 2 shows SEM micrographs of the Sn and Sn-3Ag joints after reaction at 300°C for 3600 seconds. The platelets dispersed in the solder layer were identified as Ni_3Sn_4 by XRD (Figure 3). The Sn-3Ag solder exhibits a eutectic microstructure consisting of primary β-Sn grains and Ni_3Sn_4 platelets surrounded by fine Ag_3Sn precipitates.

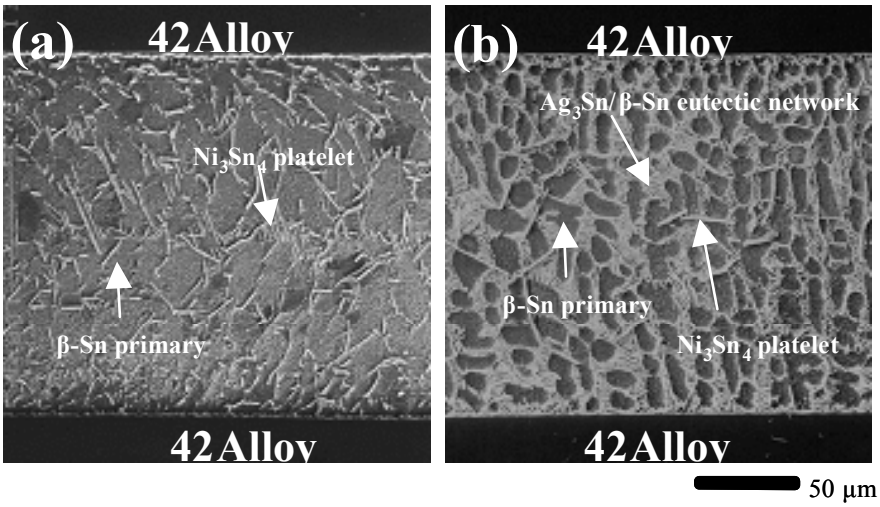

Figure 2. SEM micrographs of older/42 alloy joints; (a) pure Sn/42 alloy, (b) Sn-3Ag/42 alloy.

To assess the formation mechanism of the Ni_3Sn_4 platelets, we quenched a 42-alloy - Sn-3Ag joint by dropping it from the furnace at 250°C into an ethyl alcohol bath at –15°C. SEM and EPMA did not reveal any Ni_3Sn_4 platelets in the quenched sample. This result suggests that Ni_3Sn_4 formed during the solidification of the solder or during solid-state cooling, not at the bonding temperature.

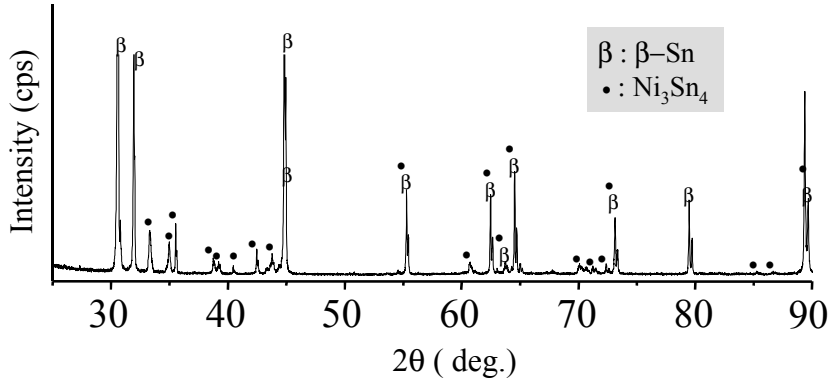

Figure 3. XRD analysis on soldered layer of Sn/42 alloy

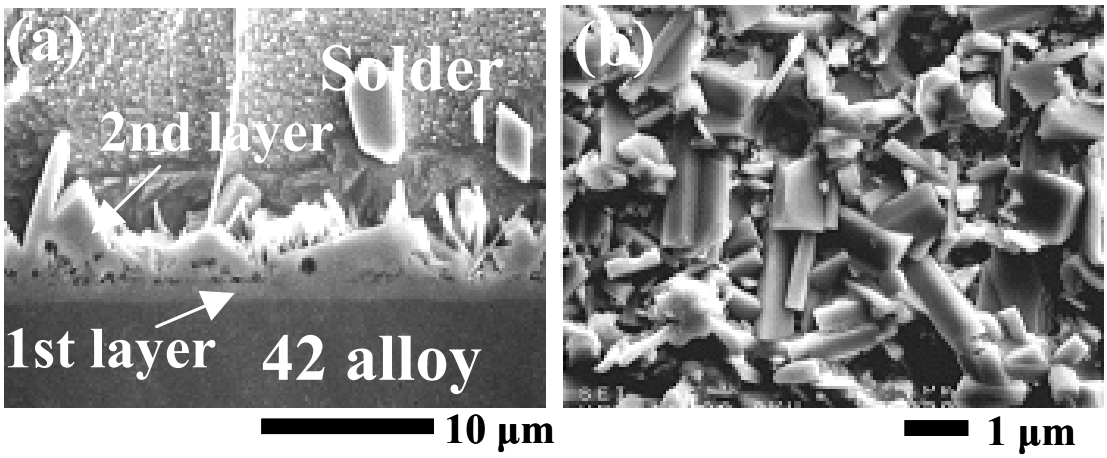

Figure 4. SEM photographs of (a) interface and (b) surface of reaction layer, obtained by etching the solder layer.

Figure 4 shows the solder-alloy interface and the surface of the reaction products (obtained after etching the solder layer) for samples bonded at 300°C for 3600 seconds. Two reaction layers appear between the 42 alloy and the solder. The thickness of the layer in contact with the 42 alloy is less than 1 µm; the layer that grows in contact with the solder consists of micron-sized platelets. According to the Fe-Sn phase diagram, at 250-300°C two reaction layers, FeSn (in contact with the alloy) and $FeSn_2$, are expected at the interface.

A line of pores appears between the two reaction layers (Figure 4a). They can form due to uncompensated diffusion across the interface. If one of the elements needed for the formation of the reaction layers diffuses faster than the other, excess vacancies will develop in the material with the highest diffusion rate. These vacancies will eventually coalesce to form pores (Kirkendall porosity). During the tensile tests, the porous interface between the reaction layers provides a weak path for crack propagation (Figure 5).

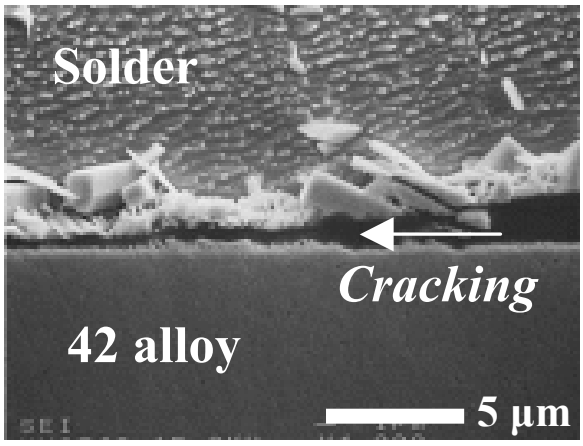

Figure 5. SEM photographs of crack propagation at the interface between the two reaction layers.

EPMA line analysis shown in Figure 6(a) indicates that the reaction layer contains only Sn and Fe (no Ni). There is little change in either Sn or Fe concentration between the two reaction layers, as expected because of the similar composition of FeSn and $FeSn_2$ (the difference in tin content is ~10 wt %) and the thinness of the reaction layers compared with the spatial resolution of EPMA. Figure 6(b) shows the XRD patterns obtained from the 42-alloy side of the fracture surface. The peaks corresponding to β-Sn, 42 alloy and $FeSn_2$ can be observed. The reaction layer of the quenched bonds was also analyzed by XRD, with similar results. Thus, the interface layer grows at the bonding temperature and is formed neither on cooling nor on solidification. Further work is needed to elucidate the formation mechanism of the reaction layer.

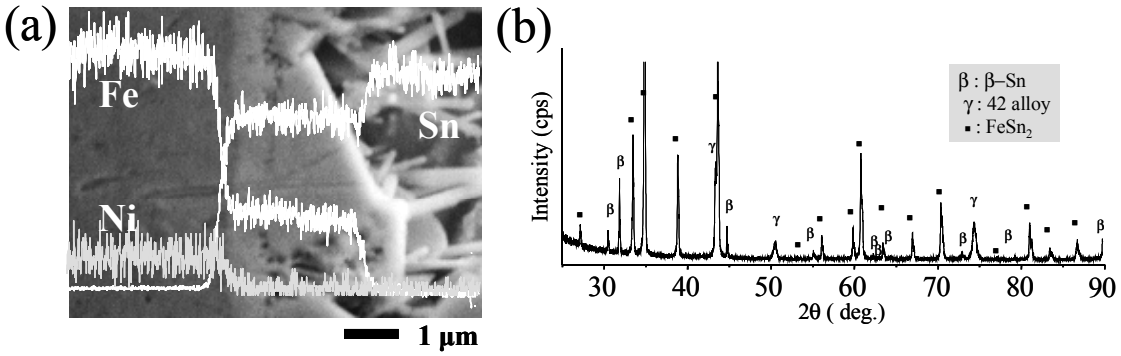

Figure 6. (a) EPMA line analysis across the reaction layer and (b) XRD analysis of fracture surface.

3.2 Influence of Bi addition on joint strength and wettability

Figure 7 shows the evolution of contact angle over time during the wetting experiments. In all systems, the contact angle decreased with time. Bi additions improved wettability. The lowest contact angle was obtained for Sn-3Ag-6Bi.

Figure 8 shows the fracture strength of the joints as a function of Bi content with or without previous Sn plating on the 42-alloy surface. In all cases, the joint strength decreased with Bi addition. SEM and EPMA revealed the segregation of Bi to the interfacial region. This segregation of Bi to the interface region seems to weaken the bond strength. Tin plating only slightly improved the interfacial strength for the Sn-3Ag-3Bi solder. However, the effect was not enough to compensate for the degradation. Joint strength did not change after annealing for 500 hours at 125ºC.

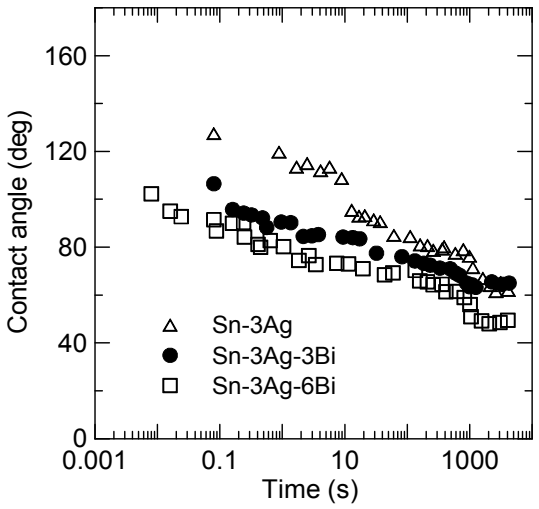

Figure 7. Contact angle as a function of time for three solders.

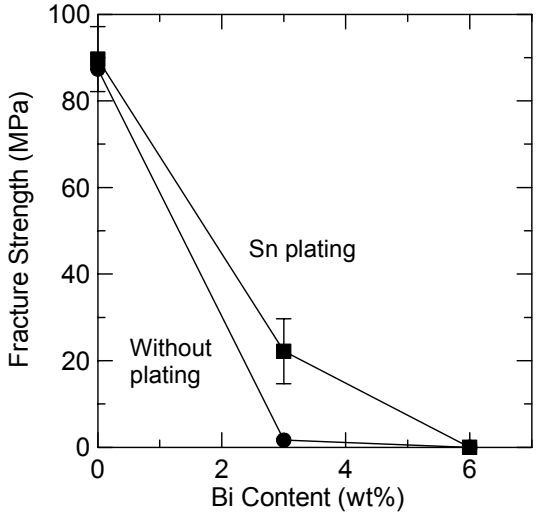

Figure 8. Joint strengths of 42-alloy joints soldered with Sn-3Ag-xBi, with and without Sn plating

4. CONCLUSIONS

In this experiment, the spreading and the interfacial microstructure in the Sn and Sn-3Ag-Bi-42-alloy system have been examined, with particular attention given to the influence of Bi on joint strength and wettability. In all cases, Ni_3Sn_4 platelets formed in the solder layer during cooling. The Sn-3Ag layer presents a eutectic microstructure consisting of primary β-Sn grains and Ni_3Sn_4 platelets surrounded by a fine network of Ag_3Sn particles. Two reaction layers form between the solder and the 42 alloy. During tensile strength tests, a crack propagates at the interface between the two reaction layers. Bismuth addition improved the wettability of the Sn-3Ag solders, but significantly decreased the bond strength (because of Bi segregation to the interfacial region).

5. ACKNOWLEDGMENTS

The authors wish to thank Mr. Kudoh for his help on plating Sn on 42 alloy. This work was partly supported the SUZUKI Foundation on Science and Technology in 2000. E. Saiz's and A. P. Tomsia's work was supported by the Director, Office of Energy Research, U.S. Department of Energy, under contract No. DE-AC03-76SF00098.

6. REFERENCES

1. K. Suganuma, J. Japan Institute of Electronics Packaging, 12, 83 (1997).

2. NCMS Lead-Free Solder Project Final Report, NCMS, Ann Arbor, MI, 1997.